

## A straightforward and quantitative approach for characterizing the photoactivation performance of optical highlighter fluorescent proteins

Jun Liu, Zhiguo Pei, Liang Wang, Zhihong Zhang, Shaoqun Zeng, and Zhen-Li Huang<sup>a)</sup>

*Britton Chance Center for Biomedical Photonics, Wuhan National Laboratory for Optoelectronics, Huazhong University of Science and Technology, Wuhan 430074, People's Republic of China*

(Received 30 July 2010; accepted 28 October 2010; published online 15 November 2010)

Characterizing the photoactivation performance of highlighter fluorescence proteins (FPs) is crucial for screening better highlighter FPs and optimizing the photoactivation efficiency of a certain highlighter FP. Currently, photoactivation contrast and half-time values of photoactivation and photobleaching processes are used for such purpose. However, the relations among these parameters are not clear, and little guidance for practical experiments could be obtained from the half-time values. Here, we show that light dose dependent fluorescence curve, which is calculated from activation-intensity-dependent photoactivation and photobleaching rates, is capable of quantifying the photoactivation performance straightforwardly. Moreover, the photoactivation contrast is easily obtained from the curve. © 2010 American Institute of Physics. [doi:10.1063/1.3518471]

The rapid development of fluorescence labeling technologies and advanced fluorescence imaging techniques provides great opportunities for noninvasive study of protein dynamics in living cells. Visualization of protein location and movement within and between cellular compartments with high spatial and temporal resolution is now made possible with the use of time-lapse fluorescence imaging and super-resolution microscopy.<sup>1</sup> In these techniques, site-specific protein labeling of subcellular compartments with high photoactivation contrast is required, which eventually leads to the advent of a unique class of probes, the optical highlighter fluorescent proteins (FPs), including photoactivatable, photoconvertible, and photoswitchable FPs.

Practically, an activation laser is typically employed to selectively activate the highlighter FPs within a cell, followed by conventional fluorescence imaging with a different laser from the one used for activation. A highlighted subcellular region with bright signals over dark backgrounds, i.e., a high level of photoactivation contrast, was generated for further protein dynamics studies.<sup>2,3</sup> Note that the photoactivation contrast is calculated from the fluorescence before and after the photoactivation. Obviously, the selection of good highlighter FPs and the optimization of the activation process are both crucial for maximizing the photoactivation contrast.

Currently, the photoactivation performance of a highlighter FP is usually characterized with several independent parameters, including maximum photoactivation contrast and half-time values of photoactivation and photobleaching processes.<sup>4,5</sup> Unfortunately, a little or no guidance could be obtained from the half-time values for practical biological imaging experiments, and due to insufficient understanding on the interaction between highlighter FPs and the activation laser, the relations among the maximum photoactivation contrast and the half-time values have been lacking in the scientific literature. Hence, in practical experiments, a complicated and time-consuming process is always necessary for maximizing the photoactivation contrast.<sup>6</sup> Considering these difficulties, a straightforward and quantitative approach for characterizing the photoactivation performance of high-

lighter FPs would be of great benefit to the screening of better highlighter FPs and the optimization of photoactivation efficiency for exploring complicated protein dynamics in single cells.

In this letter, we evaluate the photoactivation and photobleaching characteristics of several popular highlighter FPs under activation light with different intensity and propose a straightforward and quantitative approach for characterizing the photoactivation performance of optical highlighter fluorescent proteins.

The experiments were carried out with four representative highlighter FPs, including the PAGFP (the first photoactivatable highlighter), PAmCherry1 (the first photoactivatable protein screened with super-resolution microscopy), Dronpa (one of the better known photoswitchable highlighters), and Dendra2 (a popular green-to-red photoconvertible highlighter).<sup>2</sup> All of these highlighter FPs were expressed separately in *Escherichia coli* (*E. coli*) bacteria. Note that here, *E. coli* was chosen as the experimental platform for its structural simplicity and expression uniformity. A droplet ( $\sim 0.1 \mu\text{l}$ ) of a mixture of *E. coli* and double distilled water was dropped onto the surface of a clean glass coverslip, and left dry out for 1–2 min to avoid bacteria diffusion. The sample was then characterized with an Olympus FV1000 laser scanning confocal microscope equipped with an automatic Olympus IX 81 inverted microscope and a 60 $\times$  immersion oil apochromatic objective with numerical aperture (NA) of 1.42. The laser power at the sample was measured directly above the objective lens with an Ophir NOVA laser power monitor connected with an Ophir PD300-3W photodiode sensor. The light intensity at the sample,  $I$ , was calculated according to Habuchi *et al.*<sup>7</sup>

Activation of PAGFP and Dronpa was performed with a 405 nm laser in a selected sample region of about  $30 \times 30 \mu\text{m}^2$  at the center of the imaging area. A much larger area containing the activated PAGFP and Dronpa in its center was carried out with the 488 nm laser line from an argon ion laser and the emitted fluorescence was detected with a wavelength range of 495–585 nm. The Dronpa-expressing *E. coli* was first photobleached by the 488 nm laser at  $0.30 \text{ MW/cm}^2$  for  $400 \mu\text{s}$  from the fluorescent ionized state. For Dendra2 and PAmCherry1, the activation was car-

<sup>a)</sup>Electronic mail: leo@mail.hust.edu.cn.

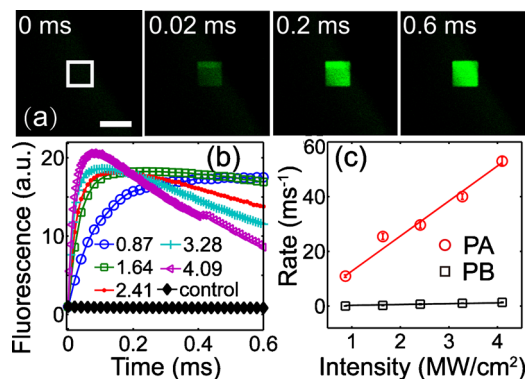


FIG. 1. (Color online) Photoactivation of PAGFP expressed in *E. coli*. (a) The fluorescence images taken at different integrated activation durations shown in the upper left corner of the images. Scale bar: 50  $\mu\text{m}$ . (b) The fluorescence curves of PAGFP under different activation intensities ( $\text{MW}/\text{cm}^2$ ). The data represent mean pixel values in the activated area and were normalized to the initial value. Time dependent fluorescence from control sample (*E. coli* without PAGFP expression) is also presented for comparison. (c) The PA and PB rates of PAGFP as a function of the activation intensity. The solid lines represent the best linear fit.

ried out with the same 405 nm laser and similar sample dimensions, while the 543 nm laser line of the green HeNe laser was used for the subsequent fluorescence imaging. The emitted fluorescence from Dendra2 and PAmCherry1 was detected between the spectral range of 560–660 nm. All the fluorescent images ( $256 \times 256$  pixels, 12 bits, bitmap) were collected under identical photomultiplier tube high voltage (700 V) and pixel integration time (2  $\mu\text{s}/\text{pixel}$ ). According to Kremers *et al.*, the excitation laser power was adjusted to yield  $\sim 200$  counts in the initial fluorescence.<sup>8</sup> The power and wavelength used for imaging the photoactivated FPs were PAGFP, 0.958  $\text{W}/\text{cm}^2$  (488 nm), Dronpa, 0.958  $\text{W}/\text{cm}^2$  (488 nm), Dendra2, 15.46  $\text{W}/\text{cm}^2$  (543 nm), and PAmCherry1, 21.16  $\text{W}/\text{cm}^2$  (543 nm), respectively. The activation duration was adjusted inversely to the activation intensity to guarantee sufficient data sampling for further curve fitting. For fluorescence imaging, the laser intensity was controlled to have negligible photobleaching effects to the activated FPs. All the photoactivation experiments were repeated 5–10 times to minimize the effects from laser power and fluorescence intensity fluctuation. *E. coli* bacteria without highlighter FP expression were used as internal control. The fluorescence images were analyzed using the software provided by the confocal system, FLUOVIEW 1.5 and MATLAB R2009B.

We first characterized the photoactivation behavior of PAGFP under different activation intensities. The fluorescence images [Fig. 1(a)] and curves [Fig. 1(b)] represent the density changes of the activated PAGFP molecules during the photoactivation process. It is clear from Fig. 1(b) that under higher activation intensities, the number of activated molecules increases and then disappears more rapidly. Interestingly, the maximum fluorescence increase after photoactivation was found to be  $\sim 20$ -fold for the PAGFP-expressing *E. coli* [Fig. 1(b)], showing a much lower photoactivation efficiency than that in PAGFP-expressing COS-7 cells ( $>60$ -fold).<sup>9</sup> Moreover, the photoactivation (PA) and photobleaching (PB) rates of PAGFP [Fig. 1(c)] were obtained from a double-exponential fitting of the corresponding fluorescence curves in Fig. 1(b).<sup>10,11</sup> We found that the dependence of PA and PB rates on the activation intensity is almost

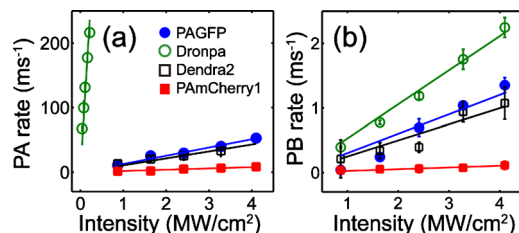


FIG. 2. (Color online) The dependence of PA and PB rates on the activation intensity. The solid lines represent the best linear fit.

linear and the PA rates are much larger than the PB rates (see more details in the following discussions). As for comparison, under similar activation conditions no fluorescence increase was observed from *E. coli* without expressing PAGFP.

We measured the activation-intensity-dependent PA and PB rates of the other three highlighter FPs (Fig. 2). It is interesting to see that Dronpa ( $1.09 \times 10^3 \text{ cm}^2/\text{MW ms}$ ) could be activated at about two orders of magnitude faster than PAGFP ( $12.81 \text{ cm}^2/\text{MW ms}$ ) and Dendra2 ( $10.78 \text{ cm}^2/\text{MW ms}$ ), demonstrating that the *cis-trans* photoisomerization in Dronpa occurs much easier than the decarboxylation in PAGFP and the backbone cleavage in Dendra2.<sup>3,12</sup> Meanwhile, the activation speed of PAmCherry1 ( $1.98 \text{ cm}^2/\text{MW ms}$ ) is about 6.5 times slower than that of PAGFP, which probably resulted from the extra oxidation process involved in the photoactivation of PAmCherry1.<sup>4,13</sup> On the other hand, the slope values of the activation-intensity-dependent PB curves of PAGFP ( $0.30 \text{ cm}^2/\text{MW ms}$ ), Dronpa ( $0.53 \text{ cm}^2/\text{MW ms}$ ), Dendra2 ( $0.25 \text{ cm}^2/\text{MW ms}$ ), and PAmCherry1 ( $0.0026 \text{ cm}^2/\text{MW ms}$ ) are 40–2000 times smaller than their corresponding PA counterparts. Note that negligible photobleaching was observed in the photoactivation of Dronpa with the low laser intensities used [Fig. 2(a)], therefore, the photobleaching rates of Dronpa in Fig. 2(b) had to be measured at much stronger activation intensity.

We hypothesized with some confidence that the slope values in Fig. 2 could be used as good parameters for characterizing the photoactivation performance of highlighter FPs. To have a better understanding on the meaning of the slope values, it is necessary to use rate equations to quantify the fluorescence trace in the photoactivation process. We expect a dual-exponential decay of the fluorescence, since both photoactivation and photobleaching effects from the activation laser are involved in the photoactivation process. Similar to the equation proposed by Chen *et al.* to describe the two-photon activation of PAGFP in the presence of photobleaching,<sup>14</sup> the dependence of fluorescence intensity ( $I_{\text{fluo}}$ ) on the activation duration ( $t$ ) could be written as

$$I_{\text{fluo}} = A \exp(k_{\text{PA}}t) + B \exp(k_{\text{PB}}t), \quad (1)$$

where  $k_{\text{PA}}$  and  $k_{\text{PB}}$  denote the activation-intensity-dependent PA and PB rates, respectively. From Fig. 2, it is easy to know that  $k_{\text{PA}} = \text{slope}_{\text{PA}}I$  and  $k_{\text{PB}} = \text{slope}_{\text{PB}}I$ . Here,  $I$  is the activation intensity. Accordingly, Eq. (1) could be rewritten as

$$I_{\text{fluo}} = A \exp(\text{slope}_{\text{PA}}It) + B \exp(\text{slope}_{\text{PB}}It). \quad (2)$$

Taking the concept of light dose,  $d = It$ , a well-accepted photophysical parameter from the field of photomedicine,<sup>15,16</sup> we have

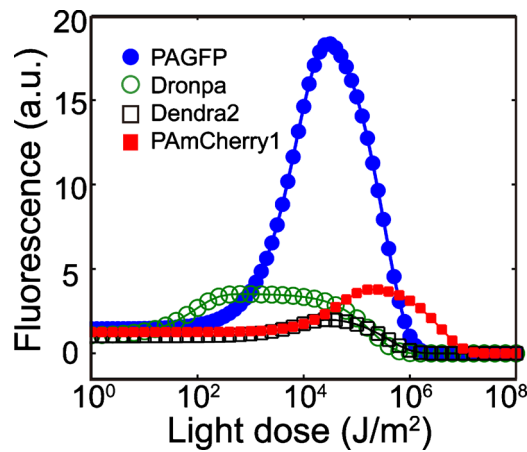


FIG. 3. (Color online) The calculated dependence of fluorescence on light dose.

$$I_{\text{fluor}} = A \exp(\text{slope}_{\text{PA}}d) + B \exp(\text{slope}_{\text{PB}}d). \quad (3)$$

With Eq. (3) and the slope values from Fig. 2, we calculated the fluorescence dynamics of the highlighter FPs as a function of light dose. It is straightforward to see from Fig. 3 that for each protein, a maximum fluorescence intensity can be acquired under an optimal light dose, which could be manipulated from both the activation duration and the intensity. Among the four highlighter FPs, Dronpa needs least light dose to achieve maximum photoactivation efficiency, indicating that Dronpa is a “photon-economic” highlighter. Moreover, when the maximum fluorescence intensity is divided by its initial value, we could easily obtain an important parameter for screening better highlighter FPs, the photoactivation contrast. However, it should be pointed out that the photoactivation contrast ratio values in our experimental conditions (*E. coli*) are significantly smaller than the reported values measured from purified proteins.<sup>2</sup> For example, the photoactivation contrast of Dendra2 was reported to be as high as 350 in the purified form,<sup>17</sup> compared to a value of less than 3 in *E. coli* (this work). To evaluate the effect of the autofluorescence from *E. coli* to the photoactivation contrast value, experiments were carried out in a special sample where *E. coli* with and without highlighter FPs expressing are presented in the same field of view. In this case, the contribution of autofluorescence background could be eliminated (or at least significantly minimized) by subtracting the total pixel intensity from the former by that from the latter with the same image area. Surprisingly, after the autofluorescence background subtraction, we found out that the increase of photoactivation contrast values in all the four highlighter FPs is less than 10%. To further verify the effectiveness of our experimental design, we characterized the photoactivation performance of purified Dendra2 proteins at a concentration of 10 mg/ml in aqueous drops in mineral oil.<sup>4</sup> Note that the same activation and imaging conditions were applied as that of the Dendra2 expressed *E. coli* sample. The photoactivation contrast was found to be  $\sim 220$ , which is much closer to the reported value of 350.<sup>17</sup> Taking the above findings into consideration, we conclude that the photoactivation contrast values measured under *E. coli* platform represent the “effective” photoactivation performance of highlighter FPs, while the values measured with purified form are much closer to the “intrinsic” photoactivation performance. To this extent, for practical cellular imaging experiments, one should

pay more efforts to characterize the effective photoactivation performance of a highlighter FP in the cell samples to be used.

In conclusion, we measured the PA and PB rates of four representative highlighter FPs (PAGFP, Dronpa, Dendra2, and PAmCherry1) under different activation intensities. We derived two useful parameters,  $\text{slope}_{\text{PA}}$  and  $\text{slope}_{\text{PB}}$ , from the activation-intensity-dependent PA and PB rates for characterizing the intrinsic properties of highlighter FPs. We calculated the light dose dependent fluorescence curves of the four highlighter FPs and showed that these curves could be used to quantify the photoactivation performance of the highlighter FPs straightforwardly. We also found out that the photoactivation contrast ratio values of the four highlighter FPs expressed in *E. coli* are significantly smaller than the reported values measured from purified proteins.

This work was supported by the National Natural Science Foundation of China (Grant Nos. 30970691, 30927001, and 30925013), the Program for New Century Excellent Talents in University of China (Grant No. NCET-08-0220 for Z.H.Z.), the Scientific Research Foundation for the Returned Overseas Chinese Scholars, the Ministry of Education of China, and the Wuhan National Laboratory for Optoelectronics. We thank Dr. G. Patterson and Dr. J. Lippincott-Schwartz for kindly providing the PAGFP plasmid, Dr. Vladislav V. Verkhusha for the PAmCherry1 plasmid, and Dr. A. Miyawaki for the Dronpa plasmid. We appreciate helpful suggestions from Dr. J. Lippincott-Schwartz, Dr. G. Patterson, Dr. K. Lukyanov, Dr. R. E. Campbell, Dr. B. Huang, and Dr. M. J. Rust, and the technical support from the Analytical and Testing Center of Huazhong University of Science and Technology.

<sup>1</sup>D. G. Spiller, C. D. Wood, D. A. Rand, and M. R. H. White, *Nature (London)* **465**, 736 (2010).

<sup>2</sup>J. Lippincott-Schwartz and G. H. Patterson, *Trends Cell Biol.* **19**, 555 (2009).

<sup>3</sup>N. C. Shaner, G. H. Patterson, and M. W. Davidson, *J. Cell Sci.* **120**, 4247 (2007).

<sup>4</sup>F. V. Subach, V. N. Malashkevich, W. D. Zencheck, H. Xiao, G. S. Filonov, S. C. Almo, and V. V. Verkhusha, *Proc. Natl. Acad. Sci. U.S.A.* **106**, 21097 (2009).

<sup>5</sup>M. Fernández-Suárez and A. Y. Ting, *Nat. Rev. Mol. Cell Biol.* **9**, 929 (2008).

<sup>6</sup>G. H. Patterson, *Current Protocols in Cell Biology* (John Wiley and Sons, Hoboken, 2008), Chap. 21.

<sup>7</sup>S. Habuchi, R. Ando, P. Dedecker, W. Verheijen, H. Mizuno, A. Miyawaki, and J. Hofkens, *Proc. Natl. Acad. Sci. U.S.A.* **102**, 9511 (2005).

<sup>8</sup>G. J. Kremers, K. L. Hazelwood, C. S. Murphy, M. W. Davidson, and D. W. Piston, *Nat. Methods* **6**, 355 (2009).

<sup>9</sup>G. H. Patterson and J. Lippincott-Schwartz, *Science* **297**, 1873 (2002).

<sup>10</sup>J. Liu, J. Chu, H. Y. Zhu, L. L. Xu, Z. H. Zhang, S. Q. Zeng, and Z. L. Huang, *Chin. Opt. Lett.* **6**, 941 (2008).

<sup>11</sup>G. H. Patterson and J. Lippincott-Schwartz, *Methods* **32**, 445 (2004).

<sup>12</sup>R. N. Day and M. W. Davidson, *Chem. Soc. Rev.* **38**, 2887 (2009).

<sup>13</sup>K. D. Piatkevich and V. V. Verkhusha, *Curr. Opin. Chem. Biol.* **14**, 23 (2010).

<sup>14</sup>Y. Chen, P. J. MacDonald, J. P. Skinner, G. H. Patterson, and J. D. Muller, *Microsc. Res. Tech.* **69**, 220 (2006).

<sup>15</sup>D. J. Robinson, H. S. de Bruijn, N. van der Veen, M. R. Stringer, S. B. Brown, and W. M. Star, *Photochem. Photobiol.* **67**, 140 (1998).

<sup>16</sup>Z. Huang, L. Li, H. Wang, X. Wand, K. Yuan, A. Meyers, L. Yang, and F. W. Hetzel, *J. Innov. Opt. Health Sci.* **2**, 73 (2009).

<sup>17</sup>N. G. Gurskaya, V. V. Verkhusha, A. S. Shcheglov, D. B. Staroverov, T. V. Chepurnykh, A. F. Fradkov, S. Lukyanov, and K. A. Lukyanov, *Nat. Biotechnol.* **24**, 461 (2006).